

Theoretical and Numerical Analysis of the Mechanical Erosion in Steam Turbine Blades. Part II

Fernando Rueda Martínez, Miguel Toledo Velázquez, Juan Abugaber Francis,
Ignacio Carvajal Mariscal, Giorgiy Polupan, José Ángel Ortega Herrera, Aldo Antonio Rueda Martínez
Applied Thermal and Hydraulic Engineering Laboratory, Lindavista, Mexico
E-mail: mtv49@yahoo.com

Received April 1, 2011; revised April 22, 2011; accepted April 30, 2011

Abstract

In the low pressure section of the steam turbines the damages are pronounced becoming remarkable in all the stages, since the generation of water liquid microparticles implies the impact on the blades having majors problems of erosion in the last stages by the increase of the humidity. In the first part of this work, the calculation presented of the transonic velocity field for the stream frictionless and the drops in the flow line, on the basis of the frictionless, two-dimensional, stationary, transonic and homogenous flow, give an approximate movement of the droplets and its accumulation on the stator blades, flowing through the steam. In order to understand the causes that originate the erosion on the blades of the last stages in low pressure section of steam turbines, the previous procedure is developed in a code in Fortran and the obtained results of velocity distribution in the output of blades that have flow conditions of wet steam are presented.

Keywords: Numerical Code, Mesh Blade, Erosion Blade, Steam Turbine, Drop Distribution

1. Introduction

In blade cascades the saturated steam flows is a nebula of droplets. Due to the accumulation that is formed on the stator blade, the erosion features in the following rotor blades is the consequence. With the water accumulation the saturated steam losses affects in the substantial mass. The impact of droplets on the blade surfaces is essentially based in the range of particles with sizes affected by the forces of inertia. These droplets cannot follow the path of the steam flow in the blade cascade.

Particularly, the effects of the saturated steam are clears by the occurrence of remarkably erosion damage. In turbines the water becomes to escape from the stator blades in form of large drops, generally toward the suction side of the following rotor blade, causing there erosion problems.

The drops distribution in a blade channel must be calculated in a parabolic distribution of velocity over the blade channel. Thus, the drop path can be solved analytically. The movement of water on the blade channel is the distribution velocity and local density of steam, and is of crucial importance. As a condition for the calculation of the drop movement, first the velocity field of the

steam in the blade cascade must be exposed in the part I of this work.

The calculation of the velocity distribution in the transonic region is necessary for the treatment of the mesh in the curvature.

For an appropriate mesh interpretation of the grade of saturated steam is essential the knowledge of the influence of the mesh geometry as well as the steam condition on the deposits of water to the stator blades profiles. The saturated steam stream in turbine stages connects the additional flow losses as well as the endangerment of the flow on the blade by drop impact erosion. Both features result of the expansion, which partially in the stator blade surface is deposited as finely fog-drop and finally a water film is formed becoming more largely secondary drop from the trailing edge.

With the help of a code in Fortran a developed computational program of calculations is accomplished and presented in the next section, whose results are communicated to the pressure and Mach number distribution, direction of flow and streamlines in the field of velocities and the drops distribution in the outlet of the stator blade channel mesh in the last pressure section of a steam turbine.

2. Procedure for the Transonic Stream in the Blade Cascade Mesh

For the calculation of the transonic stream, the time step procedure is suitable. On the basis of the conservation laws for mass, impulse and total enthalpy is compile the calculation of the stationary, frictionless, two dimensional, transonic flow in the turbine cascade according to the time in the method of the finite element. The velocity distribution determined by the calculation procedure for the frictionless stream finds the inlet into the calculation of the boundary layer on the blade surfaces and drops in the field.

The stability of the calculation can be achieved by the smoothing procedure structure in the sequence of the program, and also without the energy from other causes that dissipate generally in the zone of flow. Several inspection procedures for the results of computation are developed by the numeric approximation of time step procedure.

The consequence to receive the function values is the smooth, in order to avoid instabilities in the calculation, on which the calculation around a further interval $\Delta\tau$. The edges which can be treated simply represent the upper and lower delimitations of the profile blade range. Here the condition of periodicity must be fulfilled. It demands that the sizes in the place (i, j_s) are equal in the place (i, j_p) , as are represented in **Figure 1**.

$$f(i, j_s - 1) = f(i, j_p - 1), \quad (1)$$

$$f(i, j_p + 1) = f(i, j_s + 1). \quad (2)$$

Here the function f does not correspond to the function character σ, P, U and V . In fact, are guaranteed the values on the lines (i, j_s) and (i, j_p) as corrects. In order to exclude these deviations, in the area of the blade profiles, the values of (i, j_s) in the grid of the mesh are assigned with (i, j_p) . With the pressure on the boundary lines 1 and 2 reads the associated quantities P and σ

$$\begin{aligned} P(1) &= \frac{P_1}{\rho_1 a_1^2 M_1}, \\ \sigma(1) &= 1.0, \\ P(n) &= \frac{P_2}{\rho_1 a_1^2 M_1}, \\ \sigma(n) &= \left(\frac{P_2}{P_1} \right)^{\frac{1}{n}}. \end{aligned} \quad (3)$$

In level 1 the inflow angle, the quantity V/U pre-scribed and the amounts of U and V in such a way adapted

$$W = \sqrt{U(1)^2 + V(1)^2},$$

$$\begin{aligned} V(1)^* &= W \cdot \sin\left(\beta_1 - \frac{\pi}{2}\right), \\ U(1)^* &= W \cdot \cos\left(\beta_1 - \frac{\pi}{2}\right), \\ U(2)^* &= U(1)^*, \quad V(2)^* = V(1)^*. \end{aligned} \quad (4)$$

Here refers index (1) on the inlet level, index (2) on the following level and index (n) in each case on the outlet plane. The symbol * shows the sizes with the inflow angle β_1 . Thus, are received U and V in the level 2, therefore the exit angle

$$\beta_2 = \tan^{-1} \frac{V_2}{U_2}, \quad (5)$$

Index 1 and 2 refer the deflection condition. With a frictionless stream the velocity vector c must be zero on the blade surfaces.

$$n \cdot c = 0. \quad (6)$$

With the blade geometry also the angle θ is given on the blade surfaces. After the smoothing procedure, the associated velocity components are expressed in the blade surfaces

$$\begin{aligned} W &= \sqrt{U^2 + V^2}, \\ U^* &= W \cdot \cos \theta, \\ V^* &= W \cdot \sin \theta. \end{aligned} \quad (7)$$

The symbol * shows the sizes with the resulting velocity component and with the angle, formulated for the conditions of the blade surfaces. Same pressure in the pressure and suction side of the blade is demanded. Then is represented the function values in the following way, where $\theta(i_a - 1, j_s)$ and $\theta(i_a - 1, j_p)$ are the tangential angle in the associated place $(i_a - 1, j_s)$ and $(i_a - 1, j_p)$.

$$\begin{aligned} \sigma(i_a - 1, j_s) &= \sigma(i_a - 1, j_p), \\ P(i_a - 1, j_s) &= P(i_a - 1, j_p), \\ W_s &= \sqrt{U(i_a - 1, j_s)^2 + U(i_a - 1, j_p)^2}, \\ U^*(i_a - 1, j_p) &= W_s \cdot \cos \theta(i_a - 1, j_p), \\ V^*(i_a - 1, j_p) &= W_s \cdot \sin \theta(i_a - 1, j_p), \\ W_p &= \sqrt{U(i_a - 1, j_p)^2 + U(i_a - 1, j_s)^2}, \\ U^*(i_a - 1, j_s) &= W_p \cdot \cos \theta(i_a - 1, j_s), \\ V^*(i_a - 1, j_s) &= W_p \cdot \sin \theta(i_a - 1, j_s). \end{aligned} \quad (8)$$

The smoothing takes place with a correction step for the transition; with a time according to (t) works ($t + \Delta t$). In **Figure 1** i and j are the net indices in x and y direction. The smoothing is accomplished for the functions σ, U and V . The function f means in each case a function before the smoothing, g the same function after the smooth-

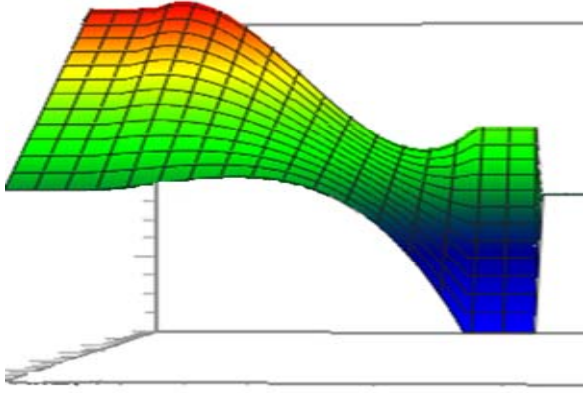


Figure 1. Designation of mesh for the zone of flow.

ing and according to the exactitude of the calculation it can be selected the size of ϕ , which is adapted to the desired computational accuracy.

$$g(i, j) = [\phi \cdot f(i, j) + f(i+1, j) + f(i-1, j) + f(i, j+1) + f(i, j-1)] / (\phi + 4) \quad (9)$$

For a two-dimensional computing area the permissible border for the time step size Δt

$$\Delta t \leq 1 / \left(\left[\frac{|c_x|}{\Delta x} + \frac{|c_y|}{\Delta y} \right] + a \cdot \sqrt{\frac{1}{\Delta x^2} + \frac{1}{\Delta y^2}} \right), \quad (10)$$

a is the local speed sound. The computer cost depends of the time step size above Δt . The organization of a more finely mesh, Δt must be selected smaller, in order to secure stability. The smoothing absorbs practically the ripples of the solution functions resulted from computing inaccuracies. In this case a polynomial of two degrees calculated according to the method of the difference squares is used. A simplification of the equation system is possible by introduction of a constant specific total enthalpy for the entire computing area. This is from the first law of thermodynamic with open stationary system and taking or adding work. The energy equation in differential form can be replaced therefore by

$$\frac{h_{tot}}{p_R / \rho_R} = \frac{\kappa}{\kappa - 1} \left(\frac{h_{tot}}{p_R / \rho_R} = 3.5 \text{ for air } \kappa = 1.4 \right). \quad (11)$$

In the proximity of the surface of the wet body the drop movement is affected by the velocity profile of the boundary layer. The integral condition for the impulse as the force equilibrium in x -direction, averaged over the boundary layer thickness δ :

$$\frac{d\delta_2}{dx} + \delta_2 \left(2 + \frac{\delta_1}{\delta_2} - M_\delta^2 \right) \frac{du_\delta/dx}{u_\delta} - \frac{c_f}{2} = 0 \quad (12)$$

with the definitions

$$\delta_1 = \int_0^\delta \left(1 - \frac{\rho u}{\rho_\delta u_\delta} \right) dy : \text{Displacement thickness.} \quad (13a)$$

$$\delta_2 = \int_0^\delta \frac{\rho u}{\rho_\delta u_\delta} \left(1 - \frac{u}{u_\delta} \right) dy : \text{Pulse loss thickness.} \quad (13b)$$

$$c_f = \tau_w / \left(\frac{\rho_\delta}{2} u_\delta^2 \right) : \text{Friction coefficient.} \quad (14)$$

$$M_\delta = \frac{u_\delta(x)}{a_\delta(x)} : \text{Local Mach number.} \quad (15)$$

The local speed sound $a_\delta(x)$ is according gas dynamics laws from the speed $u_\delta(x)$ and $M_\delta(x)$. The integral condition is kept for the kinematic energy

$$\frac{d\delta_3}{dx} + \delta_3 \left(3 + 2 \frac{\delta_4}{\delta_3} - M_\delta^2 \right) - c_D = 0 \quad (16)$$

with the definition

$$\delta_3 = \int_0^\delta \frac{\rho u}{\rho_\delta u_\delta} \left[1 - \left(\frac{u}{u_\delta} \right)^2 \right] dy : \text{Loss of energy thickness.} \quad (17)$$

$$\delta_4 = \int_0^\delta \frac{\rho u}{\rho_\delta u_\delta} \left[\left(\frac{\rho_\delta}{\rho} - 1 \right) \right] dy : \text{Density loss thickness.} \quad (18)$$

$$c_D = \frac{1}{1/2 \rho_\delta u_\delta^3} \int_0^{u_\delta} \tau du : \text{Integral of dissipations.} \quad (19)$$

$$H_{12} = \delta_1 / \delta_2 \quad \text{and} \quad H_{32} = \delta_3 / \delta_2. \quad (20)$$

In order to calculate the impact of drops on blade profiles is necessary to describe the movement of drops in a zone of flow. The general beginning for the calculation of an unsteady drop movement proceeds from the force equilibrium:

$$\sum \mathbf{K} = 0. \quad (21)$$

The sum of all forces around a drop is zero. The Equation (21) lead to the relationship

$$\mathbf{W} + \mathbf{T} = 0. \quad (22)$$

where the strength becomes

$$\mathbf{W} = c_w \cdot (\rho/2) \cdot \bar{w}_{rel} \cdot w_{rel} \cdot \pi \cdot r_T^2, \quad (23)$$

and the force of inertia is

$$\mathbf{T} = -m_T \cdot d\bar{w}_T / dt. \quad (24)$$

Here c_w is the coefficient of drag, ρ is the steam density, r_T the drop radius and w_{rel} the relative velocity between steam and drop in accordance with

$$\mathbf{w}_{rel} = \mathbf{w}_D - \mathbf{w}_T. \quad (25)$$

The drop mass m_T is calculated

$$m_T = (4/3) \pi \cdot \rho_T \cdot r_T^3 \quad (26)$$

Then, the general differential equation for drop movement

$$m_T d\mathbf{w}_T / dt = c_w \cdot (\rho/2) \cdot \mathbf{w}_{rel} \cdot w_{rel} \cdot \pi \cdot r_T^2, \quad (27)$$

the drops with a spherical shape are due to the force by the

surface tension. For the calculation of drop courses the velocity field must be given by drops moving with the help of the Equation (27). The amount of relative velocity

$$w_{rel} = \sqrt{(w_{Dx} - \dot{x})^2 + (w_{Dy} - \dot{y})^2}, \quad (28)$$

where the steam flow in the place (x, y) by the velocities w_{Dx} and w_{Dy} is given, following the relationship of the Equation (25) of the equation system: ψ

$$(8/3) \cdot (\rho_T / \rho) \cdot r_T \cdot \dot{x} - c_{w(ReT)} \cdot f_c \cdot w_{rel} \cdot (w_{Dx} - \dot{x}) = 0, \quad (29)$$

$$(8/3) \cdot (\rho_T / \rho) \cdot r_T \cdot \dot{y} - c_{w(ReT)} \cdot f_c \cdot w_{rel} \cdot (w_{Dy} - \dot{y}) = 0. \quad (30)$$

The momentary position $x(i)$ and $y(i, j)$ of the drop is admitted from the Equations (29) and (30). Index i and j refers to the x and y direction. The droplet impact on the blade surface is essentially based in the range of particles with sizes affected by the forces of inertia. These droplets cannot follow the stream of the steam flow, as is showed in **Figure 2** by the courses $\psi_{T,i}$ and $\psi_{T,i+1}$ (remarked lines) in the blade channel. These large droplets become to escape from the stator blades, generally toward the suction side of the following rotor blade, causing there erosion problems. The drop distribution in the mesh outlet level is represented on the basis of a fundamental flow pattern in a blade channel. It provides that the drops before the mesh are homogeneous distributed and that the drop velocity and steam velocity are identical to c_{T0} and c_{D0} here. The stream condition continues homogeneous by p_0 and Y_0 . The drop radius is r_{T0} . Between the two drop courses $\psi_{T,i}$ and $\psi_{T,i+1}$ in the distance $\Delta t_{0,i}$, which are identical to the steam streamlines in the mesh and two surfaces parallel to the indication level $\Delta t_{0,1}$, the water mass flow is

$$\dot{m}_{T0,i} = Y_0 \cdot \dot{m}_{0,i}, \quad (31)$$

whereby $\dot{m}_{0,i}$ is the total mass stream between the streamlines and Y_0 is the moisture content in the inlet. The number of drops in the flow is then

$$\dot{n}_{0,i} = \frac{\dot{m}_{T0,i}}{\frac{4}{3} \pi \cdot r_{T0}^3 \cdot \rho'}. \quad (32)$$

A certain part of drops which flow between the pressure side of the blade enter in contact with the profile, all these drops are closed strongly in a very thin layer on the profile surface and are concentrated finally along the flow in a narrow volume of the trailing edge, forming a water film.

The remaining drops leave from the mesh with a velocity which deviates in size and direction from the local steam velocity. In addition, they are distributed irregularly over the division. The quantity of water between the two drop courses in the level 1 is

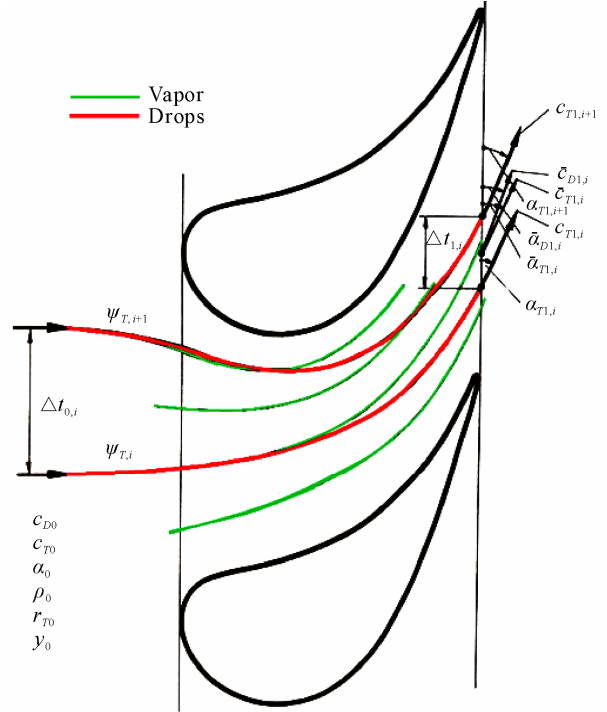


Figure 2. Nomenclature for the moisture distribution in the mesh outlet plane.

$$\dot{m}_{T1,i} = \dot{n}_{1,i} \cdot (4/3) \pi \cdot r_{T1}^3 \cdot \rho' \quad (33)$$

The mid drop course in the steam flow between the courses $\psi_{T,i}$ and $\psi_{T,i+1}$ in level 1 is:

$$\dot{m}_{D1,i} = \rho_1'' \cdot \bar{c}_{D1,i} \cdot \sin \bar{\alpha}_{D1,i} \cdot \Delta t_{1,i} \cdot \cos(\bar{\alpha}_{T1,i} - \bar{\alpha}_{D1,i}) \quad (34)$$

Steam has a medium velocity $\bar{c}_{D1,i}$ in the level 1. This direction is given by $\bar{\alpha}_{D1,i}$. The term $\cos(\bar{\alpha}_{T1,i} - \bar{\alpha}_{D1,i})$ of the steam quantity is referred to the drop course direction.

3. Particular Characteristics

The steam turbine that was used in this study gives a power of 300 MW and is analyzed a rotor blade in the last stage. The turbine is working in a thermoelectric plant of CFE installed in Estado de México, México. With real, ideal and design a value of operation [1], a graphic of steam expansion is obtained over the diagram of Mollier observed in the **Figure 3**.

The low pressure section of the steam turbine has five stages. The row of rotor step consists of 65 working blades with a measurement of 716 ± 0.5 mm each one; the profile of the rotor blade to treat is 1182SGAx and the δ_{desp} cavities on the different large of the blades measured directly over the affected zone are referred in **Figure 4**. The measurements were 30 mm for the base, 23 mm for the middle zone and 18 for the peripheral

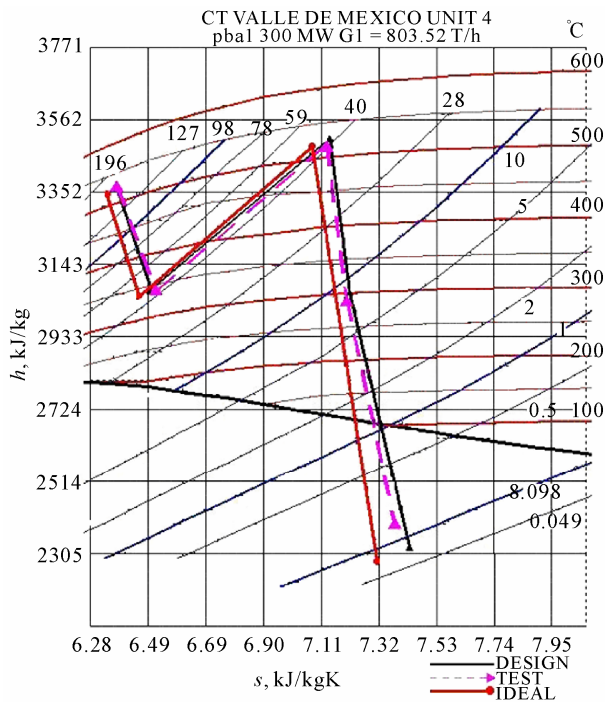


Figure 3. Steam expansion graphics of the cycle [2].



Figure 4. Damage by erosion in the working blades of the last stage in a steam turbine of 300 MW (Picture of Rueda4, 2006).

zone. The pressure that reigns in the input of rotor stage is 32.7 kPa, and the temperature is approximately 86.13°C [3].

The basic data (c_i , c_d , c_r , u , ρ , etc.) are found from the velocity relations from different enthalpies of the last stage, depending on, if it is isentropic expansion or taking in consideration losses since the design.

The humidity at the entrance of the rotor blade of 5.5% is founded in the diagram. The Figure 4 shows the

erosion in the rotor blade. The blades were heavy and the depth in their cavities formed by the erosion was measured. The original blade weight is of 5.294 kg and the actual weight, after 100,000 hours of use is 4.958 kg. The diagram of the plant where was installed the steam turbine of this work is presented in the Figure 5.

The process of steam expansion on the rows is very complicated. The drop velocities are different of the steam velocity as much by their magnitude as by their direction; in fact, it can't give a general scheme of the movement of wet steam. The path of the droplets in the channel of the blade rows can be different as is observed. In this case, the drops in the steam flow can lose their stability and be divided.

4. Results Analysis

The following measurements on the rotor blade take place: on the base, on the middle large and on the peripheral zone. In each zone was detected cavities depth with approximately 30 mm for the base, 23 mm for the middle zone and 18 mm for the peripheral zone. Like is shown in the graphic 1, the numerical data is obtained by the calculation ideal-real and design-real. It is observed that the relative impact velocity has a little difference between the comparative cases, although it is not very great, it will influence in the different stages from the impact drop velocities against the blade surface. The value of the critical radius is $r^* = 7.04 \times 10^{-3} \mu\text{m}$, therefore, the later growth of the phase begins.

The sliding velocities v are found in values close for the different cases, according to Figure 5, and decreasing of value v meaning that the velocity of the liquid phase is lower, because the droplets are bigger and the mechanic interaction causes friction, resulting in a velocity decrease. Therefore, it can observe that the liquid phase increases from the base to the blade tip. Under the

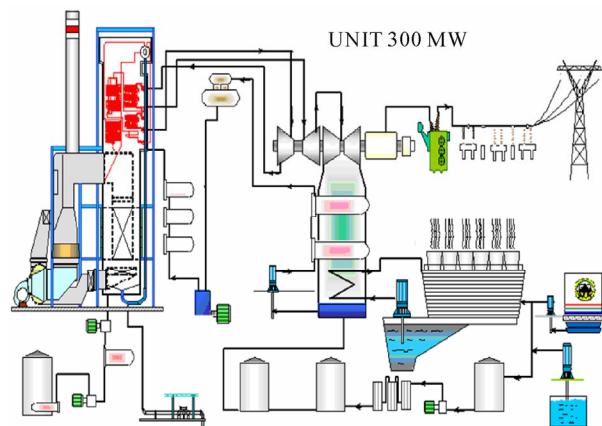


Figure 5. Plant global diagram of the U2 Steam Turbine within cycle rankine [4].

action of repetitive shocks, on the boundary surface takes the accumulation of deteriorations that are transformed into cracks by fatigue, which serve as concentrators of tensions and lead later to the destruction of isolated zones and the deterioration of the metal of the blades. This impact pressure increases little more of the double of the base to the peripheral zone, as it is possible to be observed in **Figure 6**, and in spite of having a diminution in the number of shocks per second, these shocks are stronger since the drops increase in dimension, until almost 3,5 times. The frequency of impacts will depend, in addition to the physical variables and design, of the quality of the steam in the stage, being the humidity of the last stage of approximately 5%, causing a decreasing in the performance of the turbomachinery. It is indicated that the impact pressure can depend of series of additional factors, like the metal elasticity, the drop form, the metal surface, etc.

Depending on the conditions of flow and the type of design, it will be the size of the drops and the slip coefficient that will determine the parameters that influence in the erosion of mechanical type, and will give entered to the investigation of prevention of erosion on blades in the low pressure section or, at least, to control it, since for the field of the investigation and experimentation it is necessary to have a greater knowledge of the paper that play the variables at level micro, as well as macroscopic, that causes the origin of the humidity. The macrodisperse humidity indicates that it increases, since the pressure decreases, therefore its dangerous presence increases, as were already mentioned previously.

The blade mass decreases according to the weight ob-

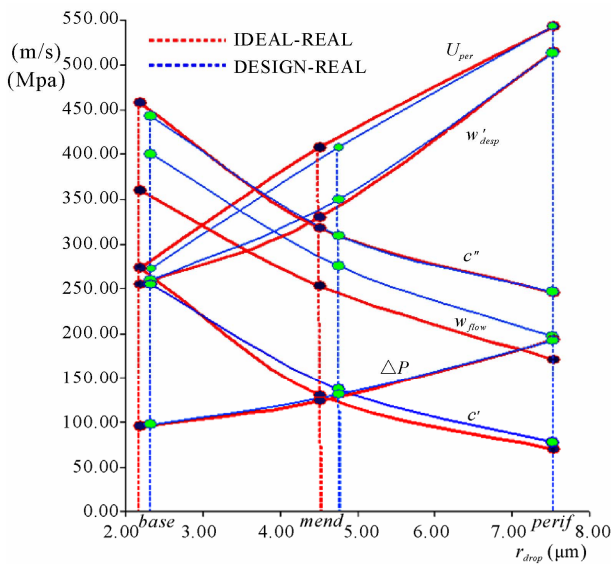


Figure 6. Graphic that relates different radii from the microparticles of liquid based on the operating velocities in the steam turbine.

tained in the laboratory in 0.336 kg and we can observe that for the ideal-real case the mass loss $\Delta m_{i-r} = 0.290$ kg, taken from the isentropic expansion and for the design-real $\Delta m_{d-r} = 0.350$ kg, because of the existence of a less enthalpy difference, having a greater closeness with the equation for the design-real case. With the comparisons elaborated in **Figure 6**, from the calculated variables that take place both for cases, ideal-real and the one of design-real (the correspondence in loss of approximated mass of the ideal data against the real ones displays a 13% difference, whereas the same loss of mass in the calculation of design against the real calculations only is of 6%), mark that is a smaller range of error in the measurement of the lost one of mass by erosion of mechanical type in the leading edges of the rotor blades for the design-real case, because in the design of the cycle in which it operates the plant they consider the losses of pressure in pipes and valves, as well as in the extractions of a stage of the section of low pressure of the turbine, whereas in the ideal designs these losses are not considered.

For the ideal case the wearing down is smaller than for the case of design. A difference of 36 grams exists (or 20% approx.) between the two forms to find the losses of mass in the blade, taking into account the total mass lost of each zone measured as showed **Figure 7**.

The flow diagram of the methodology in **Figure 8** consists of the lattice geometry and the mesh organization of the computational net. An estimated initial distribution of the searched flow parameters σ , P , U and V must be entered. With the progress of time, if the boundary conditions are kept constant, the distribution is approximately iterated more and more to the stationary solution of the zone of flow. If the difference of the flow functions is successively under a barrier which can be given, the approach to the stationary final state is terminated. The solution functions σ , P , U and V of the iterated final state, must be converted in ρ , p , c_x and c_y . The first parameter ρ_1 is selected in such a way that the given pressure P_1 of the Equation (1) of the previous Part I,

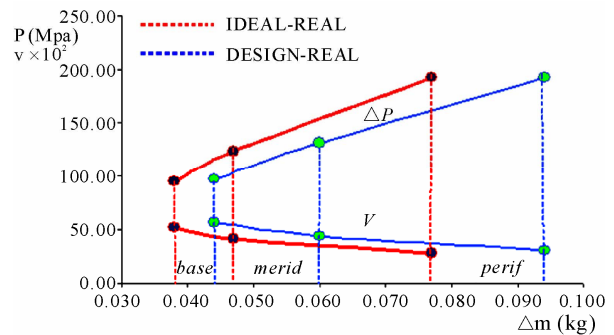


Figure 7. Graph that relates the loss of mass based on the impulse pressure and the slip coefficient v .

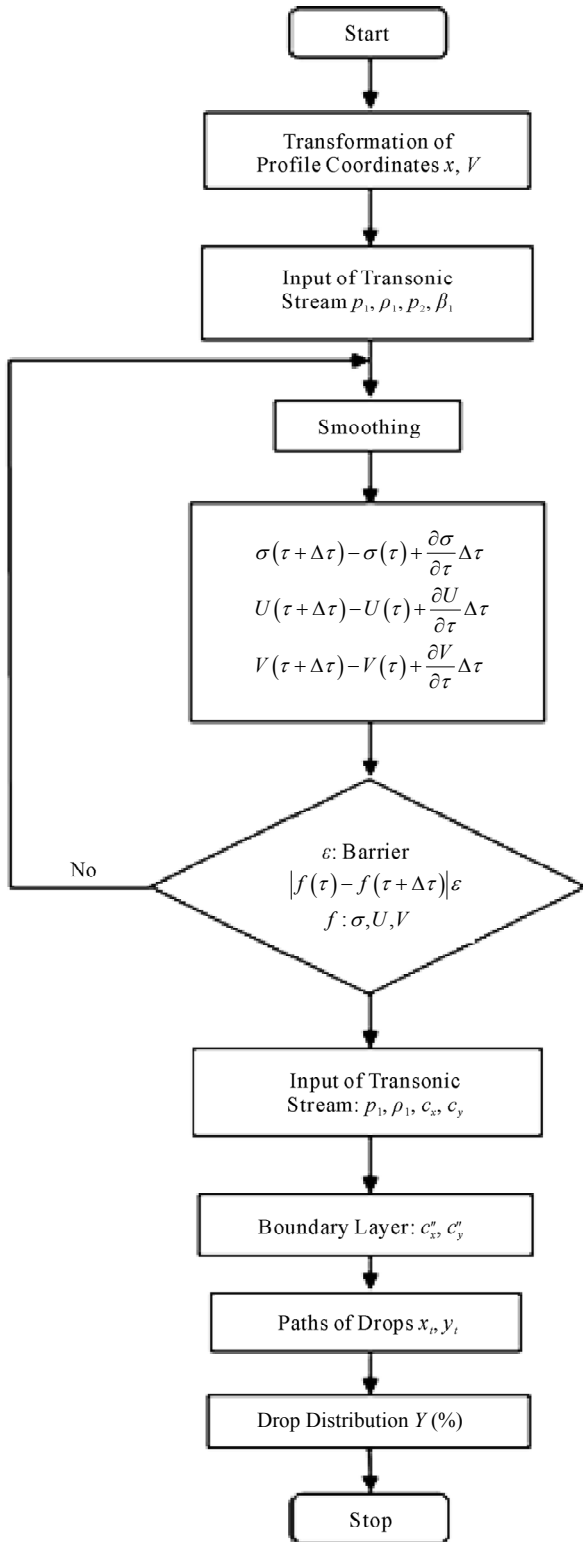


Figure 8. Flow diagram of the calculation program of droplets distribution for a stator blade of steam turbine.

fulfils the turbine design values.

The positions of drops are relevant for the calculation

of the drops distribution, and are calculated with a sub-routine. The approximate results of calculation to the stationary solution was effectuated several times and examined. For the demonstration of the liquid presence

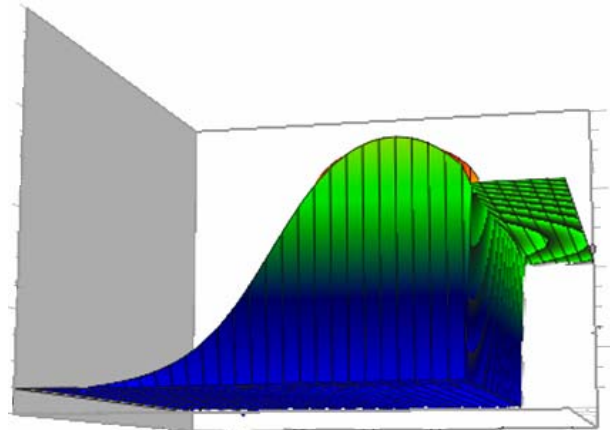


Figure 9. Behavior of axial velocity U.

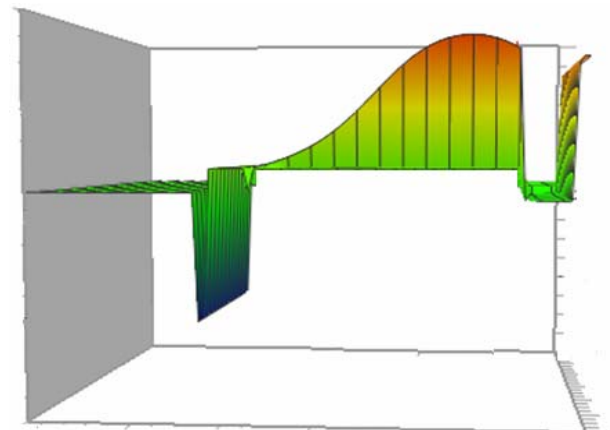


Figure 10. Behavior of peripheral velocity V.

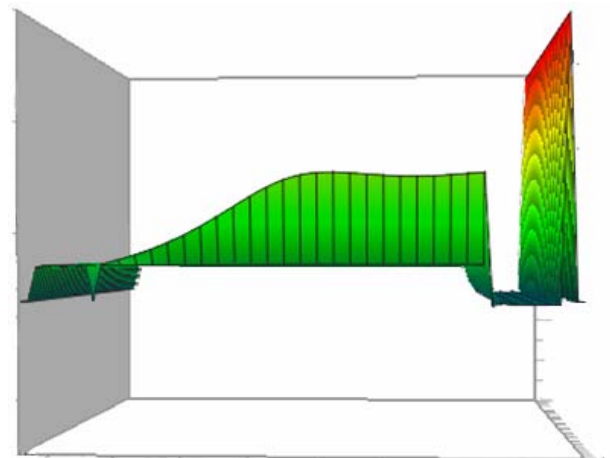


Figure 11. Velocity C toward the trailing edge.

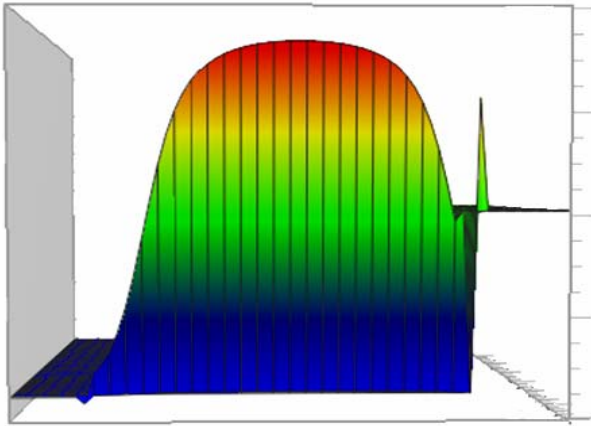


Figure 12. Inlet to exit Mach number in blade channel.

influence, a calculation with the polytropic efficiency is presented.

The results in **Figures 9 to 12** are showed. In the figures it can observe a spontaneous condensation that decelerated the Mach, axial and absolute velocity in the outlet blade channel, being the large secondary drops in the saturated steam stream are essentially responsible by the negative consequences.

The proceeding for a stator blade mesh by systematic deformations for transonic flow conditions, with respect to smaller drops of water, is introduced. Being the liquid impact erosion a major technological problem in steam turbines, the interaction of drops, droplets or clusters, plays an important role in the low pressure section. The erosion that appears on the blades by the repetitive impact of the great droplets causes damages in the surface of them and, therefore, changes in the flow conditions of the stage. For an appropriate mesh configuration of the grade of saturated steam is essential the knowledge of influence of the mesh geometry and the steam condition on the deposits of water to the stator blades profiles. With a developed code in Fortran, the calculations of drops distribution in the outlet of the stator blade mesh can be accomplished. The available information to contribute in the knowledge of the understanding of the drops distribution in the outlet stator blade mesh is analyzed.

5. Conclusions

The entire work provides information about formation and humidity distribution, as well as an evaluation with the existing theoretical treatment through a numerical development. The solutions obtained by means of the schemes of finite element show that the greater percentage of humidity begins to give when coming out of the throat of the channel, generally in the change of curvature radio of the surface of suction of the profile. Due to

this humidity concentration the properties of the fluid, the flow angle and the Mach number when coming out of the channel differ from those cascades of blades that work with superheated steam.

In the flow channel, the drops that conform the humidity are turned aside of the trajectories of the streamlines, this is due to the inertia forces that increase while the size of the drop is greater. It is in the side of pressure of the blade stator where the greater amount of drops is concentrated, these crosses through the cascade which will be accumulated and been forming a water film on the surface.

The obtained percentage of humidity increases at the outlet of the cascade, this drift that the process of accumulation of drops in the blade stator be continuous, the film that forms will be broken and greater drops will affect the edge of entrance of the rotor blade following by the suction side.

The increase in the amount of humidity is translated in losses that will become evident after certain running hours from the turbine and they will be reflected in his operation. To understand the phenomenon of erosion like a problem that is derived from the humidity existing in the channel of flow and accumulated in the stator blade, it allows improving the efficiency of the steam turbines until in an 8%.

This data is excellent to define the amount of humidity, that remains in the channel, deposited in the form of liquid film, and take the necessary measures from prevention and maintenance with respect to the problem of the erosion that arises by that reason.

6. References

- [1] "Closing report of Tests of Evaluation," Technical Subdivision, Department of Evaluations of Processes, Office of Thermal Systems, CTM-VM, CFE, October 2003.
- [2] M. F. Rueda, V. M. Toledo, S. F. Sánchez and H. J. A. Ortega, "Analysis of Erosion by Nucleation in a Steam Turbine of 300 MW," *The 2nd International Symposium on Energy Engineering, Economics and Policy*, Florida, 29 June-2 July 2010, p. 5.
- [3] "Handbook of Engineering Datas," Technical Subdivision, Department of Evaluations of Processes, Office of Thermal Systems, CTM-VM, CFE, 1980, p. 39.
- [4] M. F. Rueda, V. M. Toledo, S. F. Sánchez, G. Polupan, M. A. A. Rueda and L. G. Jarquín, "Review of Nucleation Phenomena in Steam Turbines," V Congreso Internacional de Ingeniería Electromecánica y de Sistemas, MEC100, Instituto Politécnico Nacional, México, D. F., 2008.
- [5] J. B. Young, "Wet Steam Research at Cambridge 1980-1985," EPRI Workshop on Moisture Nucleation in Steam Turbines, October 1995, pp. 11-13.